

Learning Vehicle Trajectory Uncertainty

Barak Or and Itzik Klein,

Abstract—A novel approach for vehicle tracking using a hybrid adaptive Kalman filter is proposed. The filter utilizes recurrent neural networks to learn the vehicle’s geometrical and kinematic features, which are then used in a supervised learning model to determine the actual process noise covariance in the Kalman framework. This approach addresses the limitations of traditional linear Kalman filters, which can suffer from degraded performance due to uncertainty in the vehicle kinematic trajectory modeling. Our method is evaluated and compared to other adaptive filters using the Oxford RobotCar dataset, and has shown to be effective in accurately determining the process noise covariance in real-time scenarios. Overall, this approach can be implemented in other estimation problems to improve performance.

Index Terms—Kalman filter, vehicle tracking, trajectory modeling, adaptive estimation, recurrent neural networks, long short-term memory, curvature estimation features.

I. INTRODUCTION

In many applications, accurate positioning is required. Those include, vehicle tracking tasks [1]–[8], vehicle trajectory smoothing [4], [9]–[12], autonomous driving [13], [14], advanced driver-assistance systems [15], and path planning and tracking for vehicles and robots [16], [17]. For trajectory uncertainty estimation, in [18] the authors present a vehicle trajectory prediction method that takes into account aleatoric uncertainty to improve the overall accuracy of the prediction. In [19], the authors propose a probabilistic vehicle trajectory prediction method based on a dynamic Bayesian model that integrates the driver’s intention, maneuvering behavior, and vehicle dynamics using in-vehicle sensors. The method estimates the vehicle trajectory and achieves accurate long-term predictions in both lane-keeping and lane-changing scenarios.

To achieve accurate positioning the model-based Kalman filter (KF) is widely used. One of the challenges to consider when applying a KF for tracking applications is the modeling of the vehicle trajectory, as expressed by the system matrix and associated process noise covariance. Typically, constant velocity (CV) or constant acceleration (CA) models are employed for a wide range of vehicle tracking problems [1], [12], [20]–[22]. However, these models make assumptions that may not accurately reflect real-world scenarios, where a vehicle’s velocity and acceleration may vary over time. In the CV model, the underlying assumption is that the vehicle travels with constant velocity. The addition of process noise turns the model to a nearly CV model allowing the filter to cope with varying velocity conditions. In the same manner, the CA model assumes constant vehicle acceleration and the addition of process noise turns the model to a nearly CA model

allowing the filter to cope with varying acceleration. That is, the added process noise covariance enables the filter to cope with unmodeled vehicle dynamics (for example, as additional states) or perturbations up to some order of magnitude [23].

Using the CV and CA models ensures a Gauss-Markov (GM) process and provides an optimal estimation [24], [25]. As long as the underlying model assumptions hold, the filter accuracy is satisfactory. However, in practice, the vehicle dynamics can differ from the model assumptions leading to a mismatch between the modeling and the actual behavior of the vehicle. As a consequence, the KF tracking filter performance degrades, and, in some situations, diverges. In automated vehicle perspective, it might result in a loss of information on the vehicle location that could potentially lead to an accident [26]. Therefore, model uncertainty, namely process noise covariance determination, is considered critical in the pre-processing phase of the KF [24], [27], [28].

Generally, increasing the value of the process noise covariance matrix results in the short memory behavior of the filter. In such situations, the assumption made on the vehicle’s kinematic model is less relevant, as the filter gives more weight to the external measurements when calculating the filter gain. However, in some situations, this can lead to non-optimal trajectory estimation. In contrast, setting lower values for the process noise covariance matrix leads to a long memory behavior of the filter. In such situations, the kinematic model is more dominant in the filtering process. As a result, even a small deviation from the assumed kinematic model can result in poor estimation performance and sometimes in filter divergence. To

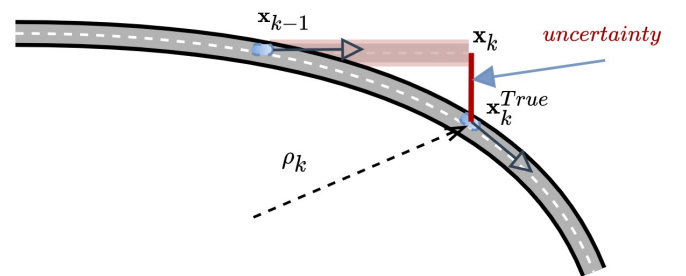


Fig. 1. Trajectory modeling error demonstration. The vehicle position at timestamp k is predicted to maintain a straight line, according to the trajectory model (CV). However, its true position at time k is along the road, where it performed a circular motion (along a circle with radius ρ) to remain on the road. This tracking error is directly caused by uncertainty in the trajectory model design (represented by the red vertical line).

cope with varying conditions along the trajectory, model-based adaptive approaches to tune the process noise covariance, were suggested in the literature [24], [29]–[32]. Among them, the common approaches are 1) the innovation-based method, where the innovation quantity is used together with the Kalman

arXiv:2206.04409v2 [cs.RO] 13 Mar 2023

gain to calibrate the matrix [33], 2) modified scaling, where the measurement noise covariance matrix is known and used to keep the trajectory uncertainty noise matrix scaled [34], and 3) generative learning, where the system transition matrix model is used to calculate and correct model error every two successive steps [23]. Although many works addressed this issue, the problem of optimal trajectory modeling by tuning the trajectory uncertainty process noise covariance is still considered unsolved [24].

Recent advancements in machine learning (ML) and deep learning (DL) techniques [35] have demonstrated state-of-the-art performance in various fields such as computer vision [36], natural language processing [37], inertial sensing [38], and autonomous underwater vehicle navigation [39], [40].

Recent works, addressing model uncertainty, explore the possibility of using ML/DL approaches. Learning approaches suggest including a loss function that contains the process noise covariance, both directly and indirectly [23]. There, the learning approach learns the covariance matrix parameters online. Yet, the resulting time to converge is too long, as the entire history of the tracking process is considered. In [9], a curve-fitting approach was proposed for tuning the trajectory uncertainty noise matrix using a neural network. However, this method requires a training set with accurate ground truth for the entire trajectory, which makes it unrealistic for real-time tracking in new environments. This is a significant limitation of the proposed method and poses a challenge to its practical implementation in real-world scenarios.

In [28], we proposed a novel hybrid learning framework for a nonlinear extended KF. This filter fuse between an inertial navigation system (INS) and a global navigation satellite system using a DL model. The DL model captures the dynamic of the system in real-time and adapts it to improve its performance. The proposed method is tested using field experiments with a quadrotor, and it was shown to improve position accuracy by 25% compared to model-based INS/GNSS fusion.

In this paper, a hybrid adaptive linear KF, based on ML algorithms and the model-based KF equations is proposed to cope with the model uncertainty in a vehicle tracking problem. Our objective is to provide a robust estimate of the process noise covariance, resulting in enhanced positioning accuracy. To that end, we implement the CV and CA models and assume the availability of position measurements received for example from radar, LiDAR, or GNSS receiver. Although an end-to-end network is simpler to implement, it does not give any intuition to the problem and acts as a black box. On the other hand, hybrid approaches rely on well-established model-based theory while adding the benefits of data-driven approaches by replacing a single operation in the model-based solution. The proposed hybrid approach consists of two steps. First, recurrent neural networks (RNNs) [41] are employed to learn the vehicle's geometrical and kinematic features, namely, the road curvature and vehicle speed. Secondly, these features are inserted into a supervised learning (SL) model providing the actual process noise covariance to use in the KF framework.

The main contributions of this paper are:

- 1) A hybrid supervised adaptive learning-based method that incorporates road curvature, vehicle speed, and noise measurement covariance as features to accurately estimate the model trajectory uncertainty.
- 2) A novel neural network structure to regresses the road curvature based on past position estimates.
- 3) Real-time implementation of a linear KF, where the learned trajectory uncertainty is utilized to optimize the model noise covariance matrix for two tracking models: CV and CA.

The proposed approach can be applied in online scenarios. To demonstrate its performance, vehicle tracking using CV and CA models is considered. The proposed approach is analyzed and compared to six other adaptive filters using the Oxford RobotCar database [42]. Results show the benefits of implementing the proposed hybrid learning model approach.

The rest of this paper is organized as follows: Section 2 deals with the problem formulation for CV and CA models and the tracking filter and its trajectory uncertainty as well as the common approaches to adapt the trajectory uncertainty noise matrix. Section 3 presents our trajectory uncertainty learning scheme including the feature engineering, dataset generation process, and online tuning scheme with the KF. Section 4 presents the results and Section 5 gives the conclusions.

II. PROBLEM FORMULATION

This section presents the tracking filter by examining three different cases of trajectory uncertainty. Additionally, the CV and CA models, along with their corresponding measurement models, are provided. Finally, various model-based adaptive approaches for determining the value of the trajectory uncertainty noise matrix in a real-time setting are discussed.

A. Tracking Filter

The linear discrete KF is presented. The filter's initial conditions are

$$\begin{aligned}\hat{\mathbf{x}}_0 &= \mathcal{E}[\mathbf{x}_0] \\ \mathbf{P}_0 &= \mathcal{E}\left[(\mathbf{x}_0 - \mathcal{E}[\mathbf{x}_0])(\mathbf{x}_0 - \mathcal{E}[\mathbf{x}_0])^T\right]\end{aligned}\quad (1)$$

where \mathbf{x}_0 is the initial state vector, $\hat{\mathbf{x}}_0$ is the initial estimate state vector, \mathbf{P}_0 is the initial covariance error, \mathcal{E} is the expected value operator, and T is the transpose operator.

The state estimate propagation is made by

$$\hat{\mathbf{x}}_k^- = \Phi \hat{\mathbf{x}}_{k-1} \quad (2)$$

where $\hat{\mathbf{x}}_k^-$ is the estimate of the current state k , $\hat{\mathbf{x}}_{k-1}$ is the estimate of the previous state ($k-1$), and Φ is the discrete system matrix.

The error covariance propagation is calculated using

$$\mathbf{P}_k^- = \Phi \mathbf{P}_{k-1} \Phi^T + \mathbf{Q}_k \quad (3)$$

where \mathbf{P}_{k-1} is the estimate from the previous state, ($k-1$), \mathbf{P}_k^- is the estimate from the current state, k , and \mathbf{Q} is the trajectory uncertainty noise matrix (covariance). When a measurement is available the state and covariance update are made according

to the following set of equations (4) – (7).

The Kalman gain is given by

$$\mathbf{K}_k = \mathbf{P}_k^- \mathbf{H}^T (\mathbf{H} \mathbf{P}_k^- \mathbf{H}^T + \mathbf{R}_k)^{-1} \quad (4)$$

where \mathbf{R} is the measurement noise covariance matrix and \mathbf{H} is the observation matrix.

The innovation vector is defined as:

$$\nu_k = \mathbf{z}_k - \mathbf{H} \hat{\mathbf{x}}_k^- \quad (5)$$

where \mathbf{z}_k is the measurement at time step k . Finally, the state estimate update is

$$\hat{\mathbf{x}}_k = \hat{\mathbf{x}}_k^- + \mathbf{K}_k \nu_k \quad (6)$$

and the error covariance update (correction) is given by

$$\mathbf{P}_k = (\mathbf{I} - \mathbf{K}_k \mathbf{H}) \mathbf{P}_k^- \quad (7)$$

The choice of \mathbf{Q} can be divided into three categories:

- 1) $\mathbf{Q} = \mathbf{0}$: might lead to a non-stabilized/optimal filter

Theorem 1. *If $\mathbf{Q}_k \rightarrow \mathbf{0}$, then the Kalman gain is a function of the weighted trajectory model, the error covariance, \mathbf{P}_{k-1} , and the measurement noise covariance only. In that manner, Eq.(4) can be rewritten as*

$$\mathbf{K}_k = \left[(\Phi \mathbf{P}_{k-1} \Phi^T)^{-1} + \mathbf{H}^T \mathbf{R}_k^{-1} \mathbf{H} \right]^{-1} \mathbf{H}^T \mathbf{R}_k^{-1} \quad (8)$$

- 2) $\|\mathbf{Q}\|_2 \rightarrow \infty$ (flat prior): leads to not considering the model, so the KF uses the measurement only.

Theorem 2. *If $\|\mathbf{Q}\|_2 \rightarrow \infty$, then the Kalman gain reduces to*

$$\mathbf{K}_k = [\mathbf{H}^T \mathbf{R}_k^{-1} \mathbf{H}]^{-1} \mathbf{H}^T \mathbf{R}_k^{-1} \quad (9)$$

and the state estimate Eq. (6) reduces to the weighted least squares estimator (LSE):

$$\hat{\mathbf{x}}_k = [\mathbf{H}^T \mathbf{R}_k^{-1} \mathbf{H}]^{-1} \mathbf{H}^T \mathbf{R}_k^{-1} \mathbf{z}_k \quad (10)$$

- 3) An arbitrary positive matrix can be set manually or using one of the methods presented in Section 2.3.

B. CV and CA Models

Any trajectory model includes some level of uncertainty. The simplest modeling approach is to set a linear trajectory motion with an additional uncertainty term. This assumption has important properties such as the Markov-Gauss process, where the current state depends only on the last state, allowing optimal implementation of the KF for accurate tracking. For example, consider an autonomous vehicle tracking problem using a CV model as demonstrated in Figure 1. In practice, the vehicle moves along a circle. The velocity vector points towards the tangential direction due to the circular motion. However, according to the assumed trajectory in the design process,, the vehicle should be moving in a straight direction. Such contradiction will lead to large positioning errors unless the process noise covariance is tuned online.

Commonly, two trajectory models are considered for vehicle motion:

- 1) **CV model:** Assumes that the vehicle moves at a constant velocity in most parts of its trajectory.

- 2) **CA model:** Assumes that the vehicle moves in a constant acceleration in most parts of its trajectory.

As the CV model is described by fewer state variables compared to CA, it is less sensitive to modeling errors. Alongside, the CA model considers the velocity changes with an additional state for the acceleration.

in the CV model, the vehicle position is modeled by

$$p_{k+1}^i = p_k^i + v_k^i \Delta t + \sqrt{q_k^i} n_k^i \quad (11)$$

while in the CA model, the vehicle position is modeled by

$$p_{k+1}^i = p_k^i + v_k^i \Delta t + \frac{1}{2} a_k^i \Delta t^2 + \sqrt{q_k^i} n_k^i \quad (12)$$

where p is the vehicle's position, v is the vehicle's velocity, a is the vehicle's acceleration, Δt is the step size (assumed to be constant), q is the uncertainty term, n is a standard Gaussian white noise, and $i \in \{x, y\}$ is the axis index.

The two-dimensional state vector of the CV model is given by

$$\mathbf{x} = \begin{bmatrix} \mathbf{p}^T & \mathbf{v}^T \end{bmatrix}^T \in \mathbb{R}^{4 \times 1} \quad (13)$$

where $\mathbf{p}^T = [p^x \ p^y]$ and $\mathbf{v}^T = [v^x \ v^y]$.

The CV model transition matrix is

$$\Phi^{CV} = \begin{bmatrix} \mathbf{I}_{2 \times 2} & \Delta t \mathbf{I}_{2 \times 2} \\ \mathbf{0} & \mathbf{I}_{2 \times 2} \end{bmatrix} \in \mathbb{R}^{4 \times 4} \quad (14)$$

where $\mathbf{I}_{n \times n}$ is the identity matrix of rank n , and the process noise covariance matrix is given by

$$\mathbf{Q}_k^{CV} = \left[\begin{array}{c|c} \mathbf{0}_{2 \times 2} & \mathbf{0}_{2 \times 2} \\ \hline \mathbf{0}_{2 \times 2} & \begin{matrix} q_k^x & 0 \\ 0 & q_k^y \end{matrix} \end{array} \right] \in \mathbb{R}^{4 \times 4} \quad (15)$$

The two-dimensional state-vector of the CA model includes the position and velocity states, as the CV model, with the addition of the acceleration state:

$$\mathbf{x} = \begin{bmatrix} \mathbf{p}^T & \mathbf{v}^T & \mathbf{a}^T \end{bmatrix}^T \in \mathbb{R}^{6 \times 1} \quad (16)$$

where $\mathbf{a}^T = [a^x \ a^y]$ and the corresponding transition matrix is given by

$$\Phi^{CA} = \begin{bmatrix} \mathbf{I}_{2 \times 2} & \Delta t \mathbf{I}_{2 \times 2} & \frac{1}{2} \Delta t^2 \mathbf{I}_{2 \times 2} \\ \mathbf{0}_{2 \times 2} & \mathbf{I}_{2 \times 2} & \Delta t \mathbf{I}_{2 \times 2} \\ \mathbf{0}_{2 \times 2} & \mathbf{0}_{2 \times 2} & \mathbf{I}_{2 \times 2} \end{bmatrix} \in \mathbb{R}^{6 \times 6} \quad (17)$$

and the trajectory noise covariance matrix is

$$\mathbf{Q}_k^{CA} = \left[\begin{array}{cc|c} \mathbf{0}_{2 \times 2} & \mathbf{0}_{2 \times 2} & \mathbf{0}_{2 \times 2} \\ \mathbf{0}_{2 \times 2} & \mathbf{0}_{2 \times 2} & \mathbf{0}_{2 \times 2} \\ \hline \mathbf{0}_{2 \times 2} & \mathbf{0}_{2 \times 2} & \begin{matrix} q_k^x & 0 \\ 0 & q_k^y \end{matrix} \end{array} \right] \in \mathbb{R}^{6 \times 6} \quad (18)$$

The state-space model, of the CV or CA methods, is defined by:

$$\mathbf{x}_{k+1} = \Phi \mathbf{x}_k + \sqrt{\mathbf{Q}_k} \mathbf{n}_k \quad (19)$$

where \mathbf{x}_k is the state vector at time step k and Φ is the dynamic transition matrix.

The error between the true state, \mathbf{x}_k^{True} , and the model state, \mathbf{x}_k , is defined by:

$$\tilde{\mathbf{x}}_k \triangleq \mathbf{x}_k - \mathbf{x}_k^{True} \quad (20)$$

To estimate the vehicle state-vector, Eq.(13) for CV or Eq.(16) for CA models, external position measurements are employed. The discrete external position measurement is given by

$$z_k^i = p_k^i + \sqrt{r_k^i} w_k^i, i \in \{x, y\} \quad (21)$$

where r_k^i is the measurement noise covariance and w_k^i is a zero-mean white Gaussian noise.

The measurement matrix for the CV model is expressed by:

$$\mathbf{H}^{CV} = \begin{bmatrix} \mathbf{I}_{2 \times 2} & \mathbf{0}_{2 \times 2} \end{bmatrix} \in \mathbb{R}^{2 \times 4} \quad (22)$$

Similarly, the measurement matrix for the CA model is defined as follows:

$$\mathbf{H}^{CA} = \begin{bmatrix} \mathbf{I}_{2 \times 2} & \mathbf{0}_{2 \times 2} & \mathbf{0}_{2 \times 2} \end{bmatrix} \in \mathbb{R}^{2 \times 6} \quad (23)$$

The corresponding measurement noise covariance matrix, for both models, is given by

$$\mathbf{R}_k^{CV} = \mathbf{R}_k^{CA} = \mathbf{R}_k = \begin{bmatrix} r_k^x & 0 \\ 0 & r_k^y \end{bmatrix} \in \mathbb{R}^{2 \times 2} \quad (24)$$

Finally, The measurement model is defined by:

$$\mathbf{z}_k = \mathbf{H}\mathbf{x}_k + \sqrt{\mathbf{R}_k} \mathbf{w}_k \quad (25)$$

where \mathbf{H} can be the CV model Eq.(22) or CA model Eq.(23) measurement matrix. Notice, as this work is focused on estimating the model uncertainty (process noise covariance), without the loss of generality, the measurement noise covariance Eq.(24) is assumed to be perfectly known.

Also, as there is no correlation between the measurement and process noises, the cross covariance matrix ($\mathcal{E}[\mathbf{n}_k \mathbf{w}_k^T]$) is assumed to be zero.

C. Model-Based Adaptive Approaches

Three commonly used model-based approaches for adaptive tuning of the process noise covariance are addressed. Those methods are described below:

- 1) **Innovation-based method.** The most common approach to estimate \mathbf{Q} in an adaptive KF framework, was suggested in [33]. This approach is based on the innovation vector (Eq.(5)) to construct the innovation matrix for a window size ξ

$$\mathbf{C}_k \triangleq \frac{1}{\xi} \sum_{j=k-\xi+1}^k \nu_j \nu_j^T \quad (26)$$

where \mathbf{C}_k is the innovation matrix. The choice of ξ is critical for the system performance: if a small window size is selected, the averaging might be insufficient to capture the relevant information. Yet, if ξ is too big, there will be a delay in the innovation estimation due to the time elapsed from the previous trajectory points.

The innovation matrix, Eq.(26), together with the Kalman gain, \mathbf{K} , are used to adapt \mathbf{Q} using:

$$\hat{\mathbf{Q}}_k = \mathbf{K}_k \mathbf{C}_k \mathbf{K}_k^T \quad (27)$$

- 2) **Generative learning.** A naive approach for learning the filter parameters (and specifically \mathbf{Q}) [23] requires access

to the full state-vector, and is generally considered inapplicable (due to difficulty in measuring all state variables). Generative learning demands the maximization of the likelihood function of all the data, using:

$$\mathbf{Q}^* = \arg \max_{\mathbf{Q}} \left\{ \begin{array}{l} -M \log [2\pi \mathbf{Q}] \\ - \sum_{k=1}^M (\mathbf{x}_k - \Phi \mathbf{x}_{k-1})^T \mathbf{Q}^{-1} (\mathbf{x}_k - \Phi \mathbf{x}_{k-1}) \end{array} \right\} \quad (28)$$

where M is the amount of samples. The optimal solution of Eq.(28) is given by

$$\mathbf{Q}_k^* = \frac{1}{M} \sum_{k=1}^M (\mathbf{x}_k - \Phi \mathbf{x}_{k-1}) (\mathbf{x}_k - \Phi \mathbf{x}_{k-1})^T \quad (29)$$

- 3) **Scaling method.** A scaling method for the covariance matrices was proposed in [43] and [44]. The Kalman gain, \mathbf{K} , depends on the ratio of \mathbf{Q} and \mathbf{R} . Hence, if one of them is known, the other can be estimated. For example, if \mathbf{R} is known, \mathbf{Q} can be estimated by satisfying the following condition for covariance matching:

$$\mathbf{H} \mathbf{P}_k^- \mathbf{H}^T + \mathbf{R}_k = \mathbf{C}_k \quad (30)$$

The core idea behind the scaling method is that if the estimated covariance of ν_k in Eq.(26) is much larger than the theoretical covariance, then \mathbf{Q} should be increased and vice versa. This deviation from the optimal value is considered using a scaling factor α_k , defined as

$$\alpha_k = \frac{\text{trace} \left(\left[\frac{1}{\xi} \sum_{j=k-\xi+1}^k \nu_j \nu_j^T \right] - \mathbf{R}_k \right)}{\text{trace} (\mathbf{H} \mathbf{P}_k^- \mathbf{H}^T)} \quad (31)$$

leading to a scaled covariance of

$$\hat{\mathbf{Q}}_k = \sqrt{\alpha_k} \hat{\mathbf{Q}}_{k-1} \quad (32)$$

III. LEARNING TRAJECTORY UNCERTAINTY

In this section, the motivation for the importance of the trajectory uncertainty matrix is described. Next, a detailed description of our proposed hybrid approach, including the learning methodology and the process of generating the datasets used in this study is given.

A. Motivation

Assume that the vehicle trajectory can be divided into a finite set of curves, $\mathbf{L}_k \in \mathcal{L}$. For each curve, the averaged curvature, averaged velocity, and measurement noise can be calculated. The curve can be represented by the vehicle estimated states:

$$\mathbf{L}_k = \{\hat{p}_i^x, \hat{p}_i^y\}_{i=k-N}^{k-1} \in \mathbb{R}^{2 \times N} \quad (33)$$

where \mathbf{L}_k is a state segment, represented by N points. Using the curvature operator, Eq.(34), the curve, as a function of the vehicle states, is mapped into a segment curvature, $\bar{\kappa}_k$:

$$\bar{\kappa}_k(\mathbf{L}_k) = \frac{1}{N} \left[\sum_{j=k}^{k+N-1} \kappa_j \right] \quad (34)$$

where κ_j is defined by

$$\kappa_j \triangleq \frac{\det(\mathbf{L}'_j, \mathbf{L}''_j)}{\|\mathbf{L}_j\|^3} \quad (35)$$

and \mathbf{L}'_k and \mathbf{L}''_k are the first and second order derivatives, respectively. From an estimation point of view, such formulation of a curve, \mathbf{L}_k , can be interpreted as a road section k provided by N points with curvature κ_k , as demonstrated in Figure 2.

Obviously, if $\kappa \rightarrow \infty$, the trajectory is a straight line and

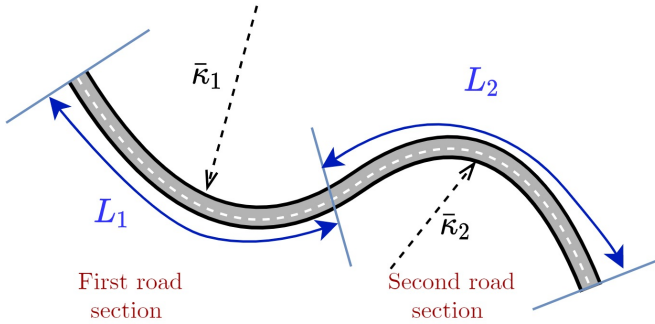


Fig. 2. A general trajectory consisting of two sections with different geometrical properties showing the length and curvature of each segment. The road curvature is defined in Eq.(35).

no compensation for the geometrical mismatch between the trajectory model and the actual vehicle trajectory should be applied. However, if the mismatch is significant, compensation for the inaccuracy of the assumed model should be applied. Hence, \mathbf{Q} should be tuned accordingly.

For example, a demonstration of the a vehicle trajectory that was set to follow a circular trajectory while the KF system model was set to follow a straight line with $\mathbf{Q} = \mathbf{0}$ is presented in Figures 3. Notice, that the KF prediction of the position vector suffered from a large error.

Thus, accurate vehicle estimation requires considering various factors such as the curvature of the vehicle's path, its speed, measurements noise, and other factors. By modeling the vehicle's trajectory as a CV or CA model, the filter designer can adjust the trajectory process noise matrix to account for these factors and their level of uncertainty. This approach can effectively handle the complexities of real-world vehicle position estimation by incorporating important features (factors) into the trajectory modeling without the need for pre-mapping road segments or using a map. This can be done in real-time, as described in the next section.

B. Proposed Approach

A novel approach is derived for online learning the trajectory model uncertainty, in terms of the process noise covariance matrix, using geometric and kinematic features. It is argued that an online calculation of such features together with a pre-trained model allows better determination of the trajectory uncertainty model, and hence, the process noise covariance matrix. In the proposed approach, presented in Figure 4, the previous N vehicle position states are inserted into a bi-directional long short-term memory (LSTM) network

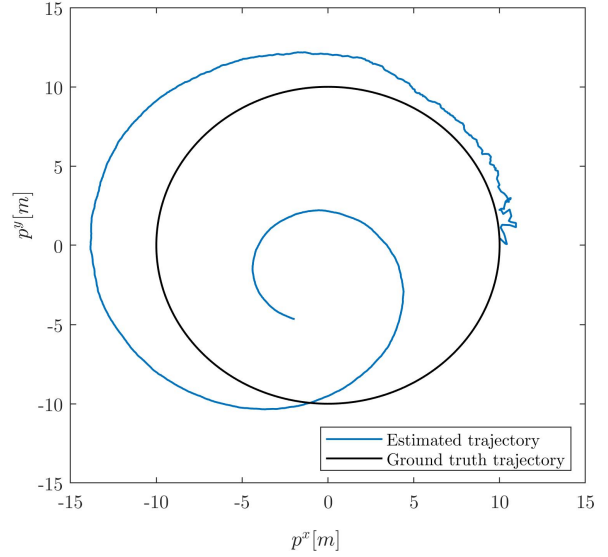


Fig. 3. Estimated and ground truth trajectories. The KF was designed with an incorrect trajectory model (the vehicle was moving in a different trajectory) and with $\mathbf{Q} = \mathbf{0}$.

to regress curvature of each trajectory segment. In parallel, the vehicle speed is calculated using the averaged estimated velocity components of the previous N states. Next, the road curvature, vehicle speed, and the measurement noise covariance, are employed as features (input) to an additional learning model (fine tree, Gaussian Process Regression (GPR), or support vector machine) to determine \mathbf{Q}_k^* . Finally, the model-based KF utilizes the adaptive learned optimal \mathbf{Q}_k^* to output the current estimated state, $\hat{\mathbf{x}}_k$. Estimating the curvature, $\hat{\kappa}$, in

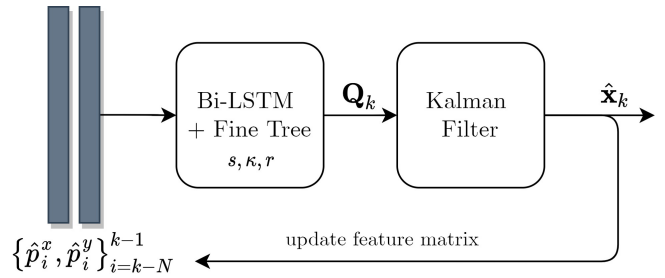


Fig. 4. block diagram of the proposed approach. N previous estimated position states are inserted into a bi-directional LSTM to regress the road curvature. The road curvature, vehicle speed, and the measurement noise covariance, are employed as features (input) to an additional learning model to determine \mathbf{Q}_k^* .

real-time vehicle tracking scenarios is not a trivial task, as the measured vehicle position and their estimates are noisy. Hence, an LSTM network was suggested to estimate the averaged curvature along a curve [45]; specifically, a bi-directional LSTM (Bi-LSTM), as described below. The curvature alone is not sufficient for tuning \mathbf{Q}_k ; therefore, two additional features are considered: 1) the measurement noise covariance and 2) the vehicle speed. These three features are combined into an ML model to determine the optimal \mathbf{Q}_k according to the last

N measurements and their estimate.

C. Learning Framework

The proposed learning framework has two steps: 1) The Bi-LSTM model used for online curvature learning 2) A feature-based SL model to estimate the process noise covariance. Here, the curvature from step 1) is used as one of the features. The proposed learning framework is illustrated in Figure 5.

1) Bi-LSTM based model for online curvature learning:

A DL-based model to generalize the geometric curvature property was designed. The main advantage of using DL is the generalization capability of intrinsic properties appearing in sequential data. The LSTM is a modification of the vanilla RNN, where feedback connections are added. Every LSTM unit with input (α_t) contains a cell (C_t), an input gate (i_t), an output gate (o_t), and a forget gate (f_t). The cell's output (h_t) is usually flattened and inserted into fully connected layers. The cell remembers values over intervals and the three gates regulate the flow of information in and out of the cell, as shown in Figure 6.

Generally, when using an LSTM network, the information passes only backward, where only casual time-dependent properties are calculated (only past information). One method to circumvent this is to pass the information forward through an additional layer, thereby allowing the network to capture additional information. This approach is known as the bi-directional LSTM (Bi-LSTM) [45] and is illustrated in Figure 7. Here, two time blocks are presented for two successive time steps, each with two LSTM blocks consisting of 100 units. One passes information forward and the other passes information backward. Their output is combined using a Sigmoid activation function to obtain their final output (m), inserted into a fully connected layer with 30 hidden units. An example on how to produce an adaptive learning curvature module is provided in Figure 8. The figure shows a circle with a predefined radius, equals to $10[m]$ (black line). The measurement noise magnitude was set to $1[m^2]$ in both x and y directions, and the vehicle speed was set to $10[m/s]$. Applying the KF (Eq.(2)-(7)), created the estimated trajectory (blue). Each 20 samples along the circle were stored with their respective optimal κ^* , as the ground truth label. By repeating this procedure a dataset was created.

2) *Learning models configuration:* Three types of features are used as input to the SL model:

1) Road curvature (as described in the previous subsection):

$$\hat{\kappa}_k = f_{Bi-LSTM} \left(\{\mathbf{x}_j\}_{j=k-N}^{k-1} \right) \quad (36)$$

where κ_k is the road curvature at time k .

2) Vehicle speed:

$$\hat{s}_k = \sqrt{(\hat{v}_k^x)^2 + (\hat{v}_k^y)^2} \quad (37)$$

where \hat{s}_k is the estimated vehicle speed calculated using the estimated velocity components at time k .

3) Measurement noise covariance:

$$\mathbf{R}_k = \begin{bmatrix} r & 0 \\ 0 & r \end{bmatrix} \quad (38)$$

where r is a know constant (for the entire scenario) noise variance .

The SL model's output is q^* :

$$q_k^* = f_{SL}(\hat{\kappa}, r, \hat{s}) \quad (39)$$

where f_{SL} is the applied learning algorithm.

3) *Learning algorithm summary:* Algorithm 1 summarizes the online tuning process of \mathbf{Q}_k , using both the Bi-LSTM network and the SL model, embedded in the model-based KF framework. In step 5, \mathbf{Q}_k is calculated using the vehicle speed, the measurement noise covariance, and the curvature estimation. An hedging mechanism enforces \mathbf{Q}_k as a positive diagonal matrix. Finally, the KF is updated and the states are stored. Step 5 expresses the proposed learning framework including the Bi-LSTM-based model and the SL model. Figure 9 shows Algorithm 1, steps 2-5, including the network structure. The general flow of the algorithm is summarized in Figure 5.

Algorithm 1 SL-based model for online tuning of \mathbf{Q}_k

Input: $\mathbf{x}_0, \mathbf{P}_0, \mathbf{Q}_0, \mathbf{R}, \Phi, \mathbf{H}, \mathbf{z}, \xi$

Output: $\hat{\mathbf{x}}_k$

- 1: Initialization: $\hat{\mathbf{x}}_0 = \mathbf{0}, \hat{\mathbf{Q}}_1 = \mathbf{Q}_0$
 - LOOP Process*
 - 2: **for** $k = 1$ to M **do**
 - 3: Propagate
 $\hat{\mathbf{x}}_k^-, \mathbf{P}_k^- = f(\Phi, \hat{\mathbf{x}}_{k-1}, \mathbf{P}_{k-1}^-, \hat{\mathbf{Q}}_k)$
 - 4: Calculate gain
 $\mathbf{K}_k = f(\mathbf{P}_k^-, \mathbf{H}, \mathbf{R})$
 - 5: Estimating speed
 $\hat{s}_k = \sqrt{(\hat{v}_k^x)^2 + (\hat{v}_k^y)^2}$
 - 6: **if** $k > \xi$ **then**
 - 7: Update $\hat{\mathbf{Q}}_k$
 $\hat{\mathbf{Q}}_k = f_{SL}(s, r, \{\mathbf{x}_j\}_{j=k-\xi+1}^k)$
 - 8: Hedging \mathbf{Q}
 $\hat{\mathbf{Q}}_k \leftarrow \hat{\mathbf{Q}}_k \odot \mathbf{I}$
 $[Q_{ij}]_k \leftarrow [Q_{ij}]_k \mathcal{I}_{\{[Q_{ij}]_k > 0\}}$
 - 9: **else**
 - 10: $\mathbf{Q}_k = \mathbf{Q}_0$
 - 11: **end if**
 - 12: Update
 $\hat{\mathbf{x}}_k, \mathbf{P}_k^+ = f(\hat{\mathbf{x}}_k^-, \mathbf{K}_k, \mathbf{z}_k, \mathbf{H}, \hat{\mathbf{x}}_{k-1}, \mathbf{P}_{k-1}^-, \hat{\mathbf{Q}}_k)$
 - 13: Return $\hat{\mathbf{x}}_k$
 - 14: **end for**
-

D. Datasets

To establish the relationship between vehicle speed, measurement noise, road curvature, and their optimal \mathbf{Q}^* matrix, the following assumptions were made:

- 1) Fixed altitude: All vehicle's trajectories are represented in two dimensions.
- 2) All vehicle's trajectories can be represented as a superposition of curves, each with corresponding curvatures κ_k .
- 3) Vehicle speed values vary between $2[m/s]$ and $40[m/s]$.

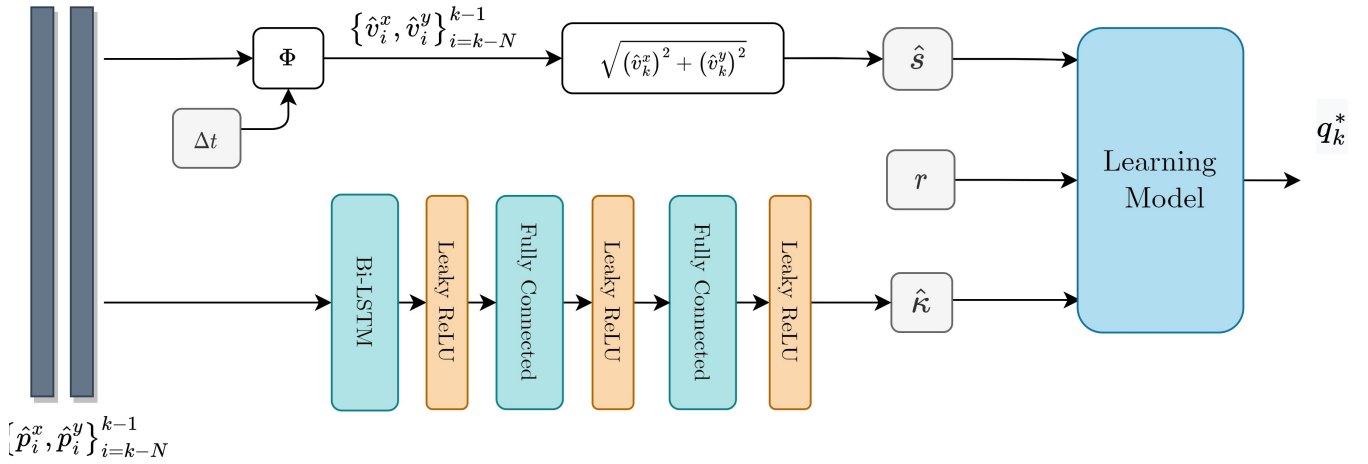


Fig. 5. The proposed learning model consists of two stages: 1) a Bi-LSTM model to regress the road curvature (κ) and 2) the three features speed (s), noise magnitude (r), and curvature, are plugged into a learning algorithm to regress the process noise covariance

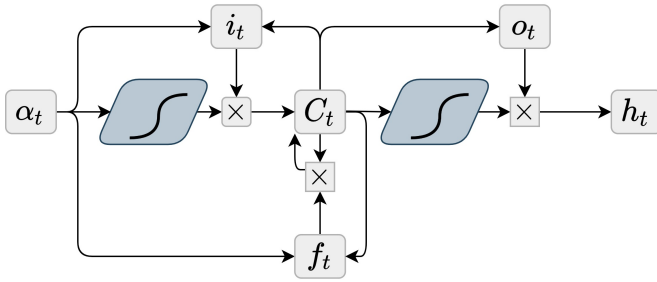


Fig. 6. LSTM unit with input, forget, and output gates.

- 4) Measurement noise variance is identical in both directions such that $r_x = r_y = r$, and noise is assumed to be zero mean white Gaussian noise.
- 5) The KF step-size is constant.

Following these assumptions, we constructed circular trajectories with different radius lengths ($1/\kappa$), measurement noise, and speed, as provided in Table 1. The circles were obtained using the following circular trajectory model:

$$p_k^x = (1/\kappa) \cos(\omega t_k) \quad (40)$$

$$p_k^y = (1/\kappa) \sin(\omega t_k) \quad (41)$$

where t_k is the time propagated by

$$t_k = t_{k-1} + \Delta t \quad (42)$$

and the angular velocity, ω , is defined by the road's curvature, κ , and the vehicle's speed, s , as

$$\omega = s\kappa. \quad (43)$$

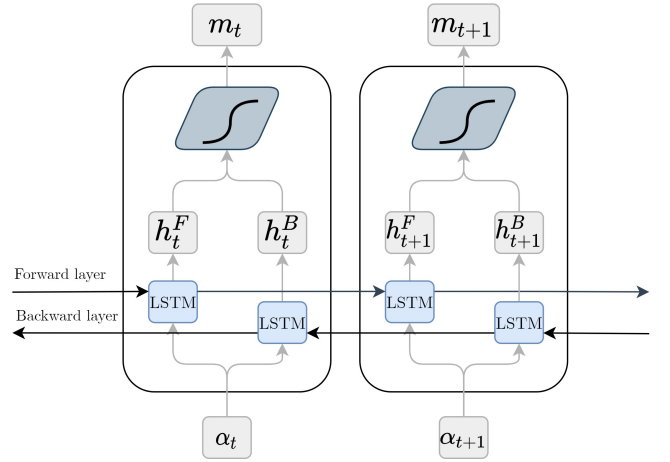


Fig. 7. Illustration of a bi-directional LSTM model. The output of the forward layer (h_t^F) is combined with the output of the backward layer (h_t^B) using a Sigmoid activation function.

Eqs.(40)-(43) combined with the KF (Eqs. (1)-(7)) were simulated once for the CV model (Eq.(14),(15),(22),(24)) and once for the CA model (Eq.(17),(18),(23),(24)).

Using the parameters in Table 1, a grid search for the optimal q^* value was performed. For example, the set $\{\kappa, r, s\}_j$ was run 34 times for different q candidates (the list is provided in the appendix). For each candidate, q_j , Monte-Carlo (MC) with 50 iterations was simulated to obtain an accurate calculation of the mean square error (MSE) measure.

Finally, the value that minimizes the MSE was stored with its set values as the ground truth values:

$$Q^* = \arg \min_Q \tilde{x}^T Q \tilde{x} \quad (44)$$

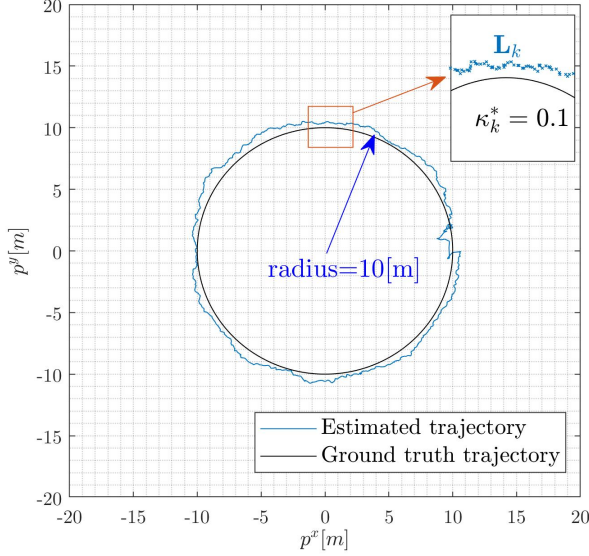


Fig. 8. An example of a trajectory included in the dataset.

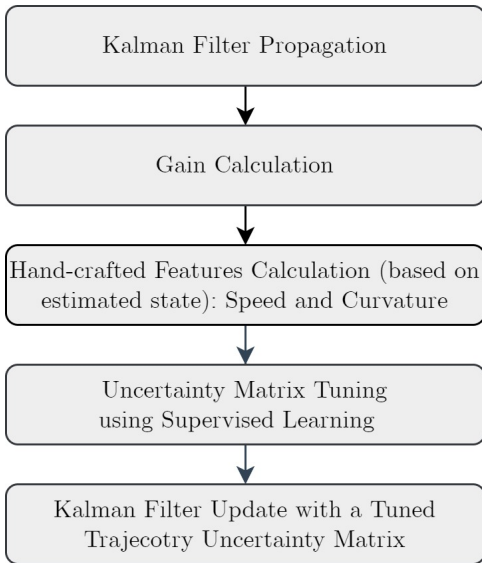


Fig. 9. The proposed algorithm follows a set of steps to estimate the trajectory uncertainty matrix. First, the state vector is propagated by using the dynamic model and the previous trajectory uncertainty matrix. Then, the Kalman gain is computed, the state vector is updated, and handcrafted features are estimated based on the state vector. Finally, using those features an SL-based model is implemented to estimate the trajectory uncertainty matrix.

where

$$\mathbf{Q} = \begin{bmatrix} \mathbf{0}_{(m-d) \times (m-d)} & \mathbf{0}_{(m-d) \times d} \\ \mathbf{0}_{d \times (m-d)} & q\mathbf{I}_{d \times d} \end{bmatrix} \in \mathbb{R}^{m \times m}, \quad (45)$$

m is the state vector dimension, and d is the physical dimension. Thus in our 2D scenarios, $d = 2$. For example, one case of finding the optimal q^* values for $\kappa = 0.05[1/m]$, $s = 10[m/s]$, $r = 1[m^2]$ in a CV trajectory model is presented in Figure 9. The optimal value obtained a position root mean square error Eq.(46) of less than $0.4[m]$ with $q^* = 0.04$.

TABLE I
FEATURE PARAMETERS USED TO CREATE THE TRAIN DATASET.

Parameter	Values Range	Value step
Speed	$2 < s < 40$ $\left[\frac{m}{s}\right]$	$\Delta s = 2$ $\left[\frac{m}{s}\right]$
Curvature	$1/200 < \kappa < 1$ $\left[\frac{1}{m}\right]$	$\Delta \kappa = 1/10$ $\left[\frac{1}{m}\right]$
Measurement noise cov.	$0.2 < r < 4$ $[m^2]$	$\Delta r = 0.2$ $[m^2]$

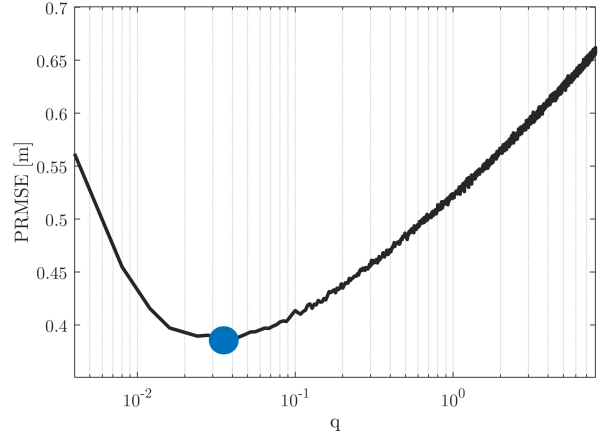


Fig. 10. An example of finding the optimal q^* in a sense of minimum PRMSE (Eq.(46)).

IV. ANALYSIS AND RESULTS

In this section, we present a comparative evaluation of model-based adaptive approaches and our suggested learning-based models. To assess the performance of the models, we utilize two error metrics as evaluation criteria:

- Position root mean square error is

$$PRMSE = \sqrt{\frac{1}{T_k} \sum_{i \in \{x,y\}} \left[\sum_{k=1}^{T_k} \left(p_k^{i, True} - \hat{p}_k^i \right)^2 \right]} \quad (46)$$

where T_k is the total time steps.

- Position mean absolute error:

$$PMAE = \frac{1}{T_k} \sum_{i \in \{x,y\}} \left[\sum_{k=1}^{T_k} \left| \left(p_k^{i, True} - \hat{p}_k^i \right) \right| \right] \quad (47)$$

A single RobotCar trajectory of 31 minutes/10[km], with varying vehicle driving scenarios, is employed as the test trajectory. This trajectory is illustrated in Figure 11.

A. Road Curvature Estimation

In the first step of the proposed learning framework, Section 3.3, the goal is to reconstruct the road curvature given a short curve ($N = 20$). To that end, another massive dataset of 240,000 examples was created. Each example contains twenty points (features), simulated along a defined circle with a known radius and its curvature (label). These examples were defined according to Table 1.

This dataset was divided in a ratio of 80/20 for the train/test procedures (192,000/48,000), where for every epoch, 24,000

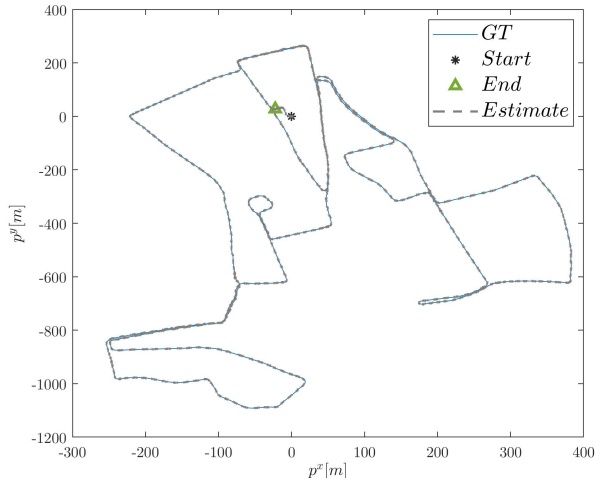


Fig. 11. A single trajectory from the Oxford RobotCar dataset with a duration of 31 minutes and 10 kilometers of vehicle driving scenarios. The estimated trajectory was obtained using the CA fine tree Bi-LSTM based $Q(r, s, \kappa)$ Regression model, where $r = 0.5[m^2]$.

shuffled examples were fed into the LSTM-based model with their respective curvature parameters. Our working environment includes: Intel i7-6700HQ CPU@2.6GHz 16GB RAM with MATLAB. The training time of the final curvature estimator elapsed about 20 minutes. The Adam optimizer [46] with a gradient threshold, for 30 epochs (8 iterations each) was employed for the training. In this setup, the trained model achieved a curvature root mean square error (RMSE) of $0.0114[m^{-1}]$ on the test set.

Six architectures for the curvature estimation task were suggested and trained:

- 1) **BiLSTM+FC**: A BiLSTM layer with 20 hidden units, followed by a fully connected (FC) layer with ten units and output layer of a unit representing the curvature size.
- 2) **BiLSTM+2FC**: Same as BiLSTM+FC with an additional FC layer with ten units.
- 3) **BiLSTM+2FC+LReLU**: Same as BiLSTM+2FC with a nonlinear activation function between the layers, leaky rectified linear unit (LReLU), to deal with the non-linearity property of the learning task.
- 4) **LSTM+FC**: One LSTM layer with 20 units followed by one FC layer.
- 5) **LSTM+2FC**: Same as LSTM+FC with an additional FC layer with 10 units.
- 6) **LSTM+2FC+LReLU**: Same as LSTM+2FC with the LReLU activation functions between the layers.

The RMSE of each model and the average running time (mean value of 1000 runs) are provided in Table 2. The best architecture, BiLSTM+2FC+LReLU, achieved a curvature RMSE of $0.0114[m^{-1}]$ on the test set.

B. Model-Based Approaches

The model-based adaptive approaches, presented in Section 2.3, were evaluated using Monte Carlo (MC) simulations with 100 iterations on the RobotCar [42] dataset (test dataset), for

various measurement noise levels as summarized in Table 3. First, the cases with $q \rightarrow 0$ (Theorem 1), which were translated for practical reasons into $q = 10^{-9}$ to avoid numerical issues, were evaluated. This case represents the high confidence level of the KF in the system modeling. There, as expected, significant position errors were obtained for all noise levels for both CV and CA models. Next, scenarios with $q \rightarrow \infty$ (Theorem 2), which were translated into $q = 10^9$ to avoid numerical issues, were examined. This case represents a flat prior, where the trajectory model is not considered, and the position error is mainly determined by measurement. The chosen constant values were the same as the measurement noise covariances: $q = r$. As expected, the RMSE was greatly improved compared to the case of $q \rightarrow 0$. Then, the adaptive model-based methods were evaluated. The innovation-based Q tuning approach, generative learning (with four/six terms along the diagonal of Q), and scaling method were implemented with a fixed window size of $\xi = 10$ as no major change in the performance for different window sizes was observed. All adaptive approaches yield better performance than $q \rightarrow 0$, $q \rightarrow \infty$, or constant values. In most cases, the lower PRMSE and PMAE were obtained for the innovation-based method with a CA model.

C. Learning-Based Approaches

In this part, the training process of the learning algorithm given the three features (speed, road curvature, and measurement noise covariance) and its integration in the model-based KF framework is addressed.

1) *SL Training Procedure*: Applying learning-based adaptive approaches can be made after they are appropriately trained. Several regression and classification models were trained and analyzed for both CV and CA datasets (Section 3.4) to determine which one of them to employ in our proposed approach. The motivation to include also the classification models, aside from the regression models, is their higher robustness as there exist a finite set of accessible values for q . The training/test procedure included the five-fold cross-validation approach [47] for obtaining robust trained models. The regression models included decision trees, linear regression, Gaussian process regression (GPR) [48], and support vector machine regression [49]. Classification models were also trained, including decision trees, k nearest neighborhood (KNN), SVM, and Naive Bayes. The training and testing were made on the dataset as defined in Section 3.4 It was observed that an optimized GPR, with a non-isotropic Matern 5/2 kernel, obtained the lowest RMSE of $0.67[m]$ and thus was selected as a possible candidate from all regression models for the CV dataset. Also, SVM with a cubic kernel was selected for the classification approach, with an accuracy of 72%. The SVM confusion matrix is presented in Figure 12, showing that most of the values were predicted correctly. For the CA dataset, a fine tree was selected as a possible candidate as it obtained the lowest RMSE of $0.83[m]$ out of all regression models. Also, SVM with a quadratic kernel was selected for the classification approach, as it obtained an accuracy of 74.5%. The SVM confusion matrix is given in Figure 13, showing that most of the values were predicted correctly.

TABLE II
DL-BASED MODELS PERFORMANCE IN ESTIMATING THE ROAD CURVATURE.

Architecture	RMSE [m^{-1}]	running time [s]
BiLSTM+FC	0.0460	0.0042
BiLSTM+2FC	0.0240	0.0042
BiLSTM+2FC+LReLU (chosen)	0.0114	0.0044
LSTM+FC	0.0257	0.0039
LSTM+2FC	0.0401	0.0042
LSTM+2FC+LReLU	0.0131	0.0042

TABLE III
COMPARISON OF SIX MODEL-BASED APPROACHES ON THE TEST DATASET WITH DIFFERENT VALUES OF THE MEASUREMENT NOISE COVARIANCE. EACH APPROACH WAS EXAMINED ON THE CV AND CA MODELS.

Model / Error metric	PRMSE [m]	PMAE [m]	PRMSE [m]	PMAE [m]	PRMSE [m]	PMAE [m]
Measurement noise cov.	$r = 0.5[m^2]$	$r = 0.5[m^2]$	$r = 2[m^2]$	$r = 2[m^2]$	$r = 4[m^2]$	$r = 4[m^2]$
CV $\mathbf{Q} \rightarrow 0$	98.4	103	125	132	143	151
CA $\mathbf{Q} \rightarrow 0$	23.6	24.5	32.0	33.0	37.5	38.4
CV $\ \mathbf{Q}\ _2 \rightarrow \infty$ (LSE)	0.99	1.12	1.99	2.25	2.82	3.19
CA $\ \mathbf{Q}\ _2 \rightarrow \infty$ (LSE)	1.00	1.12	2.00	2.25	2.82	3.18
CV constant \mathbf{Q}	0.64	0.73	1.12	1.26	1.47	1.66
CA constant \mathbf{Q}	0.62	0.70	1.13	1.27	1.53	1.72
CV innovation-based \mathbf{Q}	0.64	0.70	1.09	1.20	1.42	1.56
CA innovation-based \mathbf{Q}	0.55	0.61	0.97	1.08	1.30	1.45
CV generative learning	0.82	0.95	1.64	1.97	2.30	2.80
CA generative learning	0.82	0.96	1.64	1.98	2.31	2.83
CV scaling method	0.57	0.60	1.01	1.09	1.35	1.46
CA scaling method	0.61	0.65	1.09	1.18	1.45	1.57

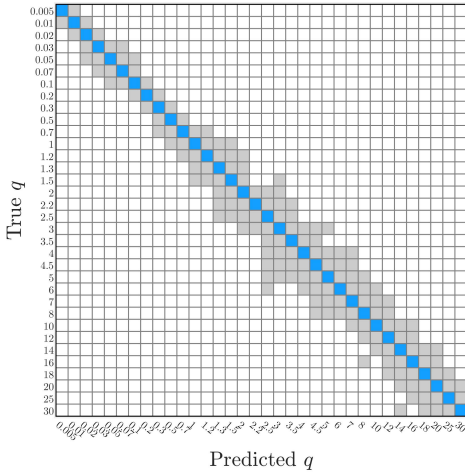


Fig. 12. Confusion matrix for SVM classifier with a cubic kernel, where the problem is formulated as a classification task (CV dataset).

2) *Integrating the ML models in the KF*: Eventually, these ML models are integrated in the KF in a real-time manner to predict and tune the sub-optimal \mathbf{Q}_k matrix and, thus, creating an hybrid learning algorithm. To that end, the GPR, SVM, and fine tree methods, for both CV and CA models were evaluated for two different cases:

- Using only two features: the measurement noise covariance (r) and speed (s). In that manner, the Bi-LSTM network is not required in the process.
- The same two features from the first case with the

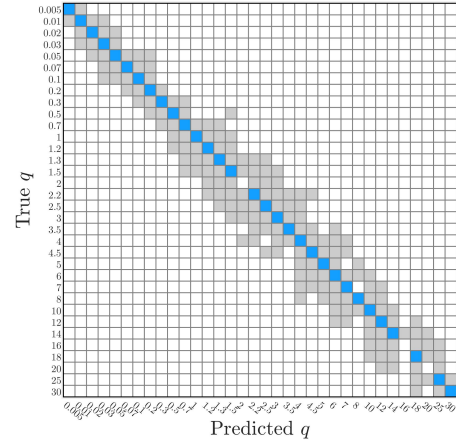


Fig. 13. Confusion matrix for the SVM classifier with a quadratic kernel, where the problem is formulated as a classification task (CA dataset).

addition of the curvature (κ) feature. In this case, the Bi-LSTM based model was plugged into the scheme, as shown in Figure 5.

Similarly to the model-based models (showing results in Table 3), the RobotCar dataset was used as the test dataset to evaluate the ML-based approaches. The learning-based approach results are summarized in Table 4.

The minimum PRMSE and PMAE for $r = 0.5[m^2]$ was obtained for the CA model with the fine tree and Bi-LSTM regression models (three features). Here, a PRMSE of $0.47[m]$ was obtained, reflecting a reduction of 13% from the CV

GPR model (PRMSE=0.54[m]). Hence, for a low covariance measurement noise of $r = 0.5[m^2]$, adding the curvature as a feature for determining \mathbf{Q}_k improves the filter's performance. In a higher measurement noise covariance, $r = 2[m^2]$, the results degrade and yield an PRMSE= 0.85[m] and PMAE=0.95 for a CA model with the SVM approach (only (s, r) as features). The reason for not considering the curvature lies in the difficulty of reconstructing the averaged curvature from a noisy series. Still, those results are lower by 12% than the one obtained using the innovation-based method with the CA model (PRMSE=0.97[m]).

Lastly, increasing the measurement noise covariance to $r = 4[m^2]$ results in a lower PRMSE =1.11[m] and PMAE=1.25[m] for a CV model with the GPR approach (a PMAE of 1.25[m] was obtained also in the CV GPR BiLSTM model). This PRMSE is lower by 14.6% than the one achieved using the CA innovation-based \mathbf{Q} approach. We also considered the case of perfect curvature, κ_{GT} , to evaluate the curvature-based models performance. The results are also summarized in Table 4, where there is a minor improvement of no more than 2% PRMSE reduction while the κ_{GT} is considered. Hence, the Bi-LSTM based curvature learning was well trained and provides an accurate curvature in a real time setting.

D. Discussion

The model-based adaptive approaches results are provided in Section 4.1 and our hybrid learning-based adaptive approaches results in Section 4.2. The performance of the adaptive model-based approaches is superior to model-based approaches with constant process noise values, as they try to capture the vehicle current dynamics and the measurement noise statistics in a real-time setting. The innovation-based model and the scaling method are better than the generative learning, as they achieved lower PRMSE and PMAE for all tested measurement noise covariance values. For $r = 0.5[m^2]$, the CA innovation-based \mathbf{Q} obtained PRMSE of 0.55[m] and PMAE of 0.61[m]. Thus, an improvements of 11% and 13% was obtained in the PRMSE and PMAE, respectively, compared to model-based approaches with constant process noise values.

The learning-based adaptive approaches were pre-trained to capture the non-linearity and other uncertainty properties; once using the relationship between the measurement noise covariance and vehicle speed and once with the addition of the road curvature as a feature. The hybrid learning-based adaptive approaches achieved better performance than the adaptive models as they consider additional learned information during the training phase. Without the curvature feature, CV GPR-based $\mathbf{Q}(r, s)$ Reg. model, obtained a PRMSE of 0.54[m] and PMAE of 0.57[m], for $r = 0.5[m^2]$. This model improves the PRMSE by 13% and the PMAE by 19% compared to model-based approaches with constant process noise values. Including the road curvature feature, the best performance for the CA model was archived with the fine tree BiLSTM-based $\mathbf{Q}(r, s, \hat{\kappa})$. It obtained a PRMSE of 0.47[m] and PMAE of 0.53[m], for $r = 0.5[m^2]$. Hence, it improves the PRMSE

by 24% and the PMAE by 24% compared to model-based approaches with the CA constant process noise values and improves the PRMSE with 14.5% and the PMAE with 13.1% compared to the adaptive model-based methods.

V. CONCLUSIONS

The proper choice of the trajectory process noise covariance matrix is critical for achieving high accuracy when implementing the discrete linear KF for vehicle tracking scenarios. The commonly used solution is to choose constant matrix parameters or to use any model-based adaptive approach. A practical hybrid ML-based framework to tune a sub-optimal covariance matrix online, was proposed. The framework combines kinematic and geometrical features, with a Bi-LSTM-based model to estimate the road curvature and an SL model utilizing it with the measurement noise covariance and vehicle speed to regress the process noise matrix.

The proposed scheme for vehicle tracking was thoroughly evaluated using extensive simulations on the RobotCar dataset. The results demonstrate the efficiency of the suggested approach as it outperforms model-based adaptive Kalman filter approaches in terms of the position RMSE. The proposed approach requires training the model only once, regardless of the specific characteristics of the vehicle's motion or the road's trajectory.

Specifically, our learning approach achieved a position RMSE lower than 0.5[m] (24% improvement compared to the best model-based approach) using a Kalman filter with a CA model, by incorporating Bi-LSTM for the road curvature regression and SVM for the process noise regression. The SVM algorithm uses only three features: vehicle speed, measurement noise covariance, and road curvature. These results demonstrate the effectiveness of the proposed method in handling the complexities of real-world vehicle tracking and pave the way for future research in this field. The proposed approach can be implemented in real-time vehicle tracking problems (for example using a standalone GNSS receiver) including autonomous vehicles, robotics platforms, or drones.

The proposed learning approach requires additional computational resources when compared to existing model-based adaptive approaches. Thus, an increase in the computational load of the system is expected. However, with the advancement in hardware and optimization techniques, this drawback can be mitigated. In future research, we aim to elaborate the proposed learning approaches by evaluating it on additional experimental data to ensure their robustness.

APPENDIX

$$\mathcal{Q} = \left\{ \begin{array}{l} 0.005, 0.01, 0.02, 0.03, 0.05, 0.07, 0.1, 0.2, \\ 0.3, 0.5, 0.7, 1, 1.2, 1.3, 1.5, 2, 2.5, 3, 3.5, 4, \\ 4.5, 5, 6, 7, 8, 10, 12, 14, 16, 18, 20, 25, 30 \end{array} \right\}$$

REFERENCES

- [1] Yaakov Bar-Shalom, X Rong Li, and Thiagalingam Kirubarajan. *Estimation with applications to tracking and navigation: theory algorithms and software*. John Wiley & Sons, 2004.
- [2] Rudolph Emil Kalman. A new approach to linear filtering and prediction problems. *Journal of Basic Engineering*, 82(1):35–45, 1960.

TABLE IV

LEARNING-BASED ADAPTIVE APPROACHES COMPARISON FOR SIX LEARNING-BASED APPROACHES ON THE TEST DATASET WITH DIFFERENT VALUES OF THE MEASUREMENT NOISE COVARIANCE. EACH RESULT IS A MEAN OF 20 REPETITIONS AND EACH APPROACH WAS EXAMINED ON THE CV AND CA MODELS.

Model / Error metric [m]	PRMSE	PMAE	PRMSE	PMAE	PRMSE	PMAE
Measurement noise covariance	$r = 0.5[m^2]$	$r = 0.5[m^2]$	$r = 2[m^2]$	$r = 2[m^2]$	$r = 4[m^2]$	$r = 4[m^2]$
CV GPR $\mathbf{Q}(r, s)$ Reg.	0.54	0.57	0.86	0.97	1.11	1.25
CV SVM $\mathbf{Q}(r, s)$ Class.	0.63	0.71	0.94	1.05	1.16	1.30
CA fine tree $\mathbf{Q}(r, s)$ Reg.	0.62	0.70	1.13	1.27	1.52	1.72
CA SVM $\mathbf{Q}(r, s)$ Class.	0.63	0.70	0.85	0.95	1.15	1.29
CV GPR BiLSTM $\mathbf{Q}(r, s, \hat{\kappa})$ Reg.	0.49	0.54	0.86	0.95	1.14	1.25
CV SVM BiLSTM $\mathbf{Q}(r, s, \hat{\kappa})$ Class.	0.51	0.55	0.91	0.99	1.22	1.32
CA fine tree BiLSTM $\mathbf{Q}(r, s, \hat{\kappa})$ Reg.	0.47	0.53	0.85	0.95	1.14	1.27
CA SVM BiLSTM $\mathbf{Q}(r, s, \hat{\kappa})$ Class.	0.50	0.56	0.90	0.99	1.20	1.33
CV GPR BiLSTM $\mathbf{Q}(r, s, \kappa_{GT})$ Reg.	0.49	0.54	0.86	0.96	1.15	1.27
CV SVM BiLSTM $\mathbf{Q}(r, s, \kappa_{GT})$ Class.	0.50	0.54	0.98	1.04	1.30	1.38
CA fine tree BiLSTM $\mathbf{Q}(r, s, \kappa_{GT})$ Reg.	0.48	0.53	0.86	0.96	1.15	1.29
CA SVM BiLSTM $\mathbf{Q}(r, s, \kappa_{GT})$ Class.	0.50	0.56	0.90	1.00	1.21	1.34

- [3] Daniel N Aloï and Oleksiy V Korniyenko. Comparative performance analysis of a Kalman filter and a modified double exponential filter for GPS-only position estimation of automotive platforms in an urban-canyon environment. *IEEE Transactions on Vehicular Technology*, 56(5):2880–2892, 2007.
- [4] Lu Xiong, Xin Xia, Yishi Lu, Wei Liu, Letian Gao, Shunhui Song, and Zhuoping Yu. IMU-based automated vehicle body sideslip angle and attitude estimation aided by GNSS using parallel adaptive Kalman filters. *IEEE Transactions on Vehicular Technology*, 69(10):10668–10680, 2020.
- [5] Danijel Pavkovic, Josko Deur, and Ilya Kolmanovsky. Adaptive kalman filter-based load torque compensator for improved si engine idle speed control. *IEEE Transactions on Control Systems Technology*, 17(1):98–110, 2008.
- [6] Zhaobo Qin, Liang Chen, Jingjing Fan, Biao Xu, Manjiang Hu, and Xin Chen. An improved real-time slip model identification method for autonomous tracked vehicles using forward trajectory prediction compensation. *IEEE Transactions on Instrumentation and Measurement*, 70:1–12, 2021.
- [7] Andrea Motroni, Alice Buffi, Paolo Nepa, and Bernardo Tellini. Sensor-fusion and tracking method for indoor vehicles with low-density uhf-rfid tags. *IEEE Transactions on Instrumentation and Measurement*, 70:1–14, 2020.
- [8] Rui Xiong, Lijing Li, Chunxi Zhang, Kun Ma, Xiaosu Yi, and Huasong Zeng. Path tracking of a four-wheel independently driven skid steer robotic vehicle through a cascaded ntsm-pid control method. *IEEE Transactions on Instrumentation and Measurement*, 71:1–11, 2022.
- [9] Stanley Baek, Chang Liu, Paul Watta, and Yi Lu Murphey. Accurate vehicle position estimation using a Kalman filter and neural network-based approach. In *2017 IEEE Symposium Series on Computational Intelligence (SSCI)*, pages 1–8. IEEE, 2017.
- [10] Hormoz Marzbani, Hamid Khayyam, Ching Nok To, ai Võ Quoc, and Reza N Jazar. Autonomous vehicles: Autodriver algorithm and vehicle dynamics. *IEEE Transactions on Vehicular Technology*, 68(4):3201–3211, 2019.
- [11] Bingbo Cui, Xinhua Wei, Xiyuan Chen, Jinyang Li, and Lin Li. On sigma-point update of cubature kalman filter for gnss/ins under gnss-challenged environment. *IEEE Transactions on Vehicular Technology*, 68(9):8671–8682, 2019.
- [12] Barak Or, Ben-Zion Bobrovsky, and Itzik Klein. Kalman filtering with adaptive step size using a covariance-based criterion. *IEEE Transactions on Instrumentation and Measurement*, 70:1–10, 2021.
- [13] Rahul Kala and Kevin Warwick. Motion planning of autonomous vehicles in a non-autonomous vehicle environment without speed lanes. *Engineering Applications of Artificial Intelligence*, 26(5-6):1588–1601, 2013.
- [14] Omveer Sharma, Nirod C Sahoo, and Niladri B Puhana. Recent advances in motion and behavior planning techniques for software architecture of autonomous vehicles: A state-of-the-art survey. *Engineering applications of artificial intelligence*, 101:104211, 2021.
- [15] P Shunmuga Perumal, M Sujasree, Suresh Chavhan, Deepak Gupta, Venkat Mukthineni, Soorya Ram Shingekar, Ashish Khanna, and Giancarlo Fortino. An insight into crash avoidance and overtaking advice systems for autonomous vehicles: a review, challenges and solutions. *Engineering applications of artificial intelligence*, 104:104406, 2021.
- [16] Andrew Gray, Yiqi Gao, Theresa Lin, J Karl Hedrick, and Francesco Borrelli. Stochastic predictive control for semi-autonomous vehicles with an uncertain driver model. In *16th International IEEE Conference on Intelligent Transportation Systems (ITSC 2013)*, pages 2329–2334. IEEE, 2013.
- [17] Zhiqiang Zhang, Lei Zhang, Junjun Deng, Mingqiang Wang, Zhenpo Wang, and Dongpu Cao. An enabling trajectory planning scheme for lane change collision avoidance on highways. *IEEE Transactions on Intelligent Vehicles*, 2021.
- [18] Hongyu Hu, Qi Wang, Laigang Du, Ziyang Lu, and Zhenhai Gao. Vehicle trajectory prediction considering aleatoric uncertainty. *Knowledge-Based Systems*, 255:109617, 2022.
- [19] Yuande Jiang, Bing Zhu, Shun Yang, Jian Zhao, and Weiwen Deng. Vehicle trajectory prediction considering driver uncertainty and vehicle dynamics based on dynamic bayesian network. *IEEE Transactions on Systems, Man, and Cybernetics: Systems*, 2022.
- [20] Mohammed M Olama, Seddik M Djouadi, Ioannis G Papageorgiou, and Charalambos D Charalambous. Position and velocity tracking in mobile networks using particle and kalman filtering with comparison. *IEEE Transactions on Vehicular Technology*, 57(2):1001–1010, 2008.
- [21] Yuchuan Fu, Changle Li, Fei Richard Yu, Tom H Luan, and Yao Zhang. A decision-making strategy for vehicle autonomous braking in emergency via deep reinforcement learning. *IEEE Transactions on Vehicular Technology*, 69(6):5876–5888, 2020.
- [22] Stephen C Stubberud, Kathleen A Kramer, and J Antonio Geremia. Online sensor modeling using a neural kalman filter. *IEEE Transactions on Instrumentation and Measurement*, 56(4):1451–1458, 2007.
- [23] Pieter Abbeel, Adam Coates, Michael Montemerlo, Andrew Y Ng, and Sebastian Thrun. Discriminative Training of Kalman Filters. In *Robotics: Science and Systems*, volume 2, page 1, 2005.
- [24] Lingyi Zhang, David Sidoti, Adam Bienkowski, Krishna R Pattipati, Yaakov Bar-Shalom, and David L Kleinman. On the identification of noise covariances and adaptive Kalman filtering: A new look at a 50 year-old problem. *IEEE Access*, 8:59362–59388, 2020.
- [25] Andrew H Jazwinski. *Stochastic processes and filtering theory*. Courier Corporation, 2007.
- [26] Julia Nilsson, Mattias Brännström, Erik Coelingh, and Jonas Fredriksson. Lane change maneuvers for automated vehicles. *IEEE Transactions on Intelligent Transportation Systems*, 18(5):1087–1096, 2016.
- [27] Antonio Artunedo, Jorge Villagra, Jorge Godoy, and Maria Dolores del Castillo. Motion planning approach considering localization uncertainty. *IEEE Transactions on Vehicular Technology*, 69(6):5983–5994, 2020.
- [28] Barak Or and Itzik Klein. A hybrid model and learning-based adaptive navigation filter. *IEEE Transactions on Instrumentation and Measurement*, pages 1–1, 2022.
- [29] Farhad Aghili and Chun-Yi Su. Robust relative navigation by integration of ICP and adaptive Kalman filter using laser scanner and IMU. *IEEE/ASME Transactions on Mechatronics*, 21(4):2015–2026, 2016.
- [30] AH Mohamed and KP Schwarz. Adaptive Kalman filtering for INS/GPS. *Journal of Geodesy*, 73(4):193–203, 1999.

- [31] Yuanxi Yang and Weiguang Gao. An optimal adaptive Kalman filter. *Journal of Geodesy*, 80(4):177–183, 2006.
- [32] Gheorghe Galben. New three-dimensional velocity motion model and composite odometry–inertial motion model for local autonomous navigation. *IEEE Transactions on Vehicular Technology*, 60(3):771–781, 2011.
- [33] Raman Mehra. On the identification of variances and adaptive Kalman filtering. *IEEE Transactions on Automatic Control*, 15(2):175–184, 1970.
- [34] Manika Saha, Ratna Ghosh, and Bhaswati Goswami. Robustness and sensitivity metrics for tuning the extended Kalman filter. *IEEE Transactions on Instrumentation and Measurement*, 63(4):964–971, 2013.
- [35] Ian Goodfellow, Yoshua Bengio, and Aaron Courville. *Deep learning*. MIT Press, 2016.
- [36] Yanming Guo, Yu Liu, Ard Oerlemans, Songyang Lao, Song Wu, and Michael S Lew. Deep learning for visual understanding: A review. *Neurocomputing*, 187:27–48, 2016.
- [37] Erik Cambria and Bebo White. Jumping NLP curves: A review of natural language processing research. *IEEE Computational Intelligence Magazine*, 9(2):48–57, 2014.
- [38] Itzik Klein. Data-driven meets navigation: Concepts, models, and experimental validation. In *2022 DGON Inertial Sensors and Systems (ISS)*, pages 1–21. IEEE, 2022.
- [39] Nadav Cohen and Itzik Klein. Beamsnet: A data-driven approach enhancing doppler velocity log measurements for autonomous underwater vehicle navigation. *Engineering Applications of Artificial Intelligence*, Vol. 114, 105216, 2022.
- [40] Barak Or and Itzik Klein. A hybrid adaptive velocity aided navigation filter with application to INS/DVL fusion. In *OCEANS 2022, Hampton Roads*, pages 1–5. IEEE, 2022.
- [41] Alex Sherstinsky. Fundamentals of recurrent neural network (rnn) and long short-term memory (lstm) network. *Physica D: Nonlinear Phenomena*, 404:132306, 2020.
- [42] Will Maddern, Geoffrey Pascoe, Chris Linegar, and Paul Newman. 1 year, 1000 km: The Oxford RobotCar dataset. *The International Journal of Robotics Research*, 36(1):3–15, 2017.
- [43] Weidong Ding, Jinling Wang, Chris Rizos, and Doug Kinlaysia. Improving adaptive Kalman estimation in GPS/INS integration. *The Journal of Navigation*, 60(3):517, 2007.
- [44] Congwei Hu, Wu Chen, Yongqi Chen, Dajie Liu, et al. Adaptive Kalman filtering for vehicle navigation. *Journal of Global Positioning Systems*, 2(1):42–47, 2003.
- [45] Felix A Gers, Jürgen Schmidhuber, and Fred Cummins. Learning to forget: Continual prediction with LSTM. *Neural Computation*, 12(10):2451–2471, 2000.
- [46] Diederik P Kingma and Jimmy Ba. Adam: A method for stochastic optimization. *arXiv preprint arXiv:1412.6980*, 2014.
- [47] Payam Refaeilzadeh, Lei Tang, and Huan Liu. Cross-validation. *Encyclopedia of Database Systems*, 5:532–538, 2009.
- [48] Matthias Seeger. Gaussian processes for machine learning. *International Journal of Neural Systems*, 14(02):69–106, 2004.
- [49] Olivier Chapelle and Vladimir Vapnik. Model selection for support vector machines. *Advances in Neural Information Processing Systems*, 12:230–236, 1999.